

A Study of Hybrid Modernized GPS and Galileo Positioning in Japan

Falin WU*, Nobuaki KUBO** and Akio YASUDA**

Abstract

The modernization of the GPS and the advent of the European Galileo will enhance the capability of quickly and correctly resolving the integer cycle carrier phase ambiguities in precise differential positioning. In this paper the performances of hybrid modernized GPS and Galileo positioning are analyzed for different scenarios by using the LAMBDA method in Japan. The scenarios include modernized GPS system, future Galileo system and combined GPS and Galileo system over different baselines. The results show that extending a present dual frequency GPS system to hybrid modernized GPS and Galileo system in future will significantly improve the capability of Real-Time Kinematic (RTK) positioning. On the short baseline very high ambiguity success rate can be easily obtained, even with a single epoch of data. On the medium baseline the ambiguity success rate could increase by the increased number of satellites and the improved satellite geometry. On the long baseline, for which differential atmospheric delays have to be dealt with, reliable instantaneous ambiguity resolution is feasible only if a stringent condition is met on either the code measurement accuracy or on the accuracy of atmospheric correction information.

Keywords: Precise Positioning, Modernized GPS, Galileo

1. Introduction

Undoubtedly, the GPS modernization program as well as the setup of the anticipated European counterpart Galileo will prove to be highly beneficial for Real-Time Kinematic (RTK) positioning. GPS Block IIR-M and IIF will both transmit the unencrypted L2 civil signal on the second carrier frequency making the tracking of this signal much easier and reliable. The modernization of the GPS and the advent of Galileo will together lead cooperatively to a truly multi-frequency civil Global Navigation Satellite System (GNSS).

This paper focuses on the performance of integral modernized GPS and Galileo positioning in Japan. In the paper, the signal structure and parameters of modernized GPS and Galileo are briefly reviewed. RTK positioning using integral modernized GPS and

Galileo are introduced. The ambiguity success rates are calculated with a geometry-based model for different scenarios using the LAMBDA method⁽¹⁾⁽⁴⁾. The scenarios chosen for analyses are introduced, and the system's performance on ambiguity resolution will be presented over time and for locations in Japan. The performance will be quantified for differential positioning over short, medium and long distances. Since only instantaneous ambiguity resolution is considered, which is based on a single epoch of data, no distinction between a moving and a stationary receiver is necessary.

2. GPS Modernization and Galileo

The modernization of GPS has been proceeding for the past several years based on discussions, recommendations, and plans that have occurred over most of

* Student Member: Tokyo University of Mercantile Marine (2-1-6, Etchujima, Koto-ku, Tokyo 135-8533)

** Member: Tokyo University of Mercantile Marine (2-1-6, Etchujima, Koto-ku, Tokyo 135-8533)

the last decade. Also, coordination, planning and activities in European Union to the implementation of the Galileo navigation satellite system have cautiously but steadily advance considerably during this same period.

2.1 GPS Modernization

2.1.1 Satellite Constellation

The original Block II and IIA operational GPS satellites have all been launched, so no modifications or changes to these satellites are possible. Seven of the GPS Block IIR replenishment satellites have been launched and six are actively now supporting the GPS operational constellation. Twenty-one of these satellites were acquired by Air Force from Lockheed Martin. Part of the current modernization plan is to modify the last twelve of these completed satellites to provide the capabilities. The civil L5 capabilities will not be incorporated into the modified IIR-M's because of a satellite prime power limitation⁽⁶⁾.

2.1.2 Signal Structure

The current constellation of GPS Block II and IIA satellites provides C/A code on L1 only, whereas the encrypted P-code is modulated on both carriers, L1 and L2. The modernized GPS will transmit two new additional coded civil signals, the civil code on the L2 frequency and the new signal at L5.

GPS Block IIR are launched since 1997 to replace the older Block II (and IIA) vehicles. A modernized version (Block IIR-M) is planned for 2003 with the C/A code and an L2 civil signal being implemented on L1 and L2, respectively. Furthermore, the military M-code is expected to be modulated on both carriers.

Albeit GPS Block IIR-M will not offer a third frequency, tracking the L2 carrier will become significantly easier and the signal-to-noise ratio on the second frequency will improve. This fact is also important for kinematic applications since ionospheric disturbances may cause loss-of-lock especially on L2 much easier for current GPS than for GPS IIR-M due to the accessible civil code on L2⁽⁶⁾.

2.2 Galileo

2.2.1 Satellite Constellation

The space segment of Galileo is intended to consist of a total 30 Mean Earth Orbiting (MEO) satellites

Table 1 Parameters for Galileo satellite

Semi-major axis	a	29994 km
Inclination	i	56°
Eccentricity	e	0.0
Right ascension	Ω_0	-120°, 0°, 120°
Rate of right ascension	$\dot{\Omega}$	0.0°/day
Argument of perigee	ω	0.0°
Mean anomaly (1 st orbit plan)	M_0	-160°, 120°, ..., 120°, 160°

Table 2 Galileo carrier frequencies

Carrier	Center Frequency (MHz)
E5a(L5)	11676.45
E5b	[1196.91-1027.14]
E6	1278.750
E2-L1-E1	1575.42

configured as *Walker constellation*, i.e. distributed over three orbital planes. The altitude is 23616 km, and the inclination is 56°. Table 1 gives the almanac parameters for Galileo constellation⁽³⁾⁽⁹⁾.

2.2.2 Signal Structure

Center frequencies of Galileo are presented in Table 2. Galileo will provide ten navigation signals in Right Hand Circular Polarization in the frequency rang 1164-1215 MHz (E5a and E5b), 1215-1300 MHz (E6) and 1559-1592 MHz (E2-L1-E1), which are part of the Radio Navigation Satellite Service allocation. All the Galileo satellites will share the same nominal frequency, making use of Code Division Multiple Access (CDMA) compatible with the GPS approach.

Six signals, including three data-less channels, so-called pilot tones, are accessible to all Galileo Users on the E5a, E5b and E2-L1-E1 carrier frequencies for Open Services and Safety-of-Life Service. Two signals on E6 with encrypted ranging codes, including one data-less channel are accessible only to some dedicated users that gain access through a given Commercial Service provider. Finally, two signals with encrypted ranging codes and data are accessible to authorized users of the Public Regulated Service⁽³⁾.

3. Hybrid Modernized GPS and Galileo

Positioning

The measured ranges, by pseudorange and carrier phase respectively, are related to the unknown parameters via the following generic measurement equations⁽⁸⁾:

$$P_{r,i}^s = \rho_r^s + d_{r,i} - d^{s,i} + \frac{f_{L1}^2}{f_i^2} I_r^s + T_r^s + e_{r,i}^s \dots\dots\dots (1)$$

$$\Phi_{r,i}^s = \rho_r^s + \delta_{r,i} - \delta^{s,i} - \frac{f_{L1}^2}{f_i^2} I_r^s + T_r^s + \lambda_i N_{r,i}^s + \epsilon_{r,i}^s \dots\dots\dots (2)$$

where Φ and P are the carrier phase and pseudorange, respectively; ρ is the geometric range from satellite s to receiver r ; i is the L-band frequency signals, $i=L1, L2, L5, E1, E5a, E5b$ and $E6$; I and T are the ionospheric and tropospheric delay, respectively; d and δ are the satellite and receiver clock error, respectively; λ and N are the wavelength and ambiguity of signal i carrier phase; ϵ and e represent the effect of receiver noise on the carrier phase and the pseudorange, respectively.

3.1 Single-Point Positioning

The linearized pseudorange measurement is given by the following:

$$\Delta\rho = G\Delta x + \Delta e \dots\dots\dots (3)$$

where $\Delta\rho$ is the vector of predicted minus actual pseudorange measurement. The vector Δx has four components, the first three are the position offset of the user from the linearization point; the fourth is the offset of the user time bias. The $m \times 4$ geometry matrix G only depends upon the line-of-sight effect. Δe is the residual error vector after the known biases have been removed.

The Dilution of Precision (DOP) is a measure for the geometrical strength of the observation model. Different types of DOP values are distinguished. Here only geometric DOP, GDOP is considered. The DOP values depend on the cofactor matrix, $Q = (G^T G)^{-1}$. The GDOP is defined as:

$$GDOP = \sqrt{\text{trace}(Q)} = \sqrt{Q_{11} + Q_{22} + Q_{33} + Q_{44}} \dots\dots\dots (4)$$

3.2 Real-Time Kinematic Positioning

3.2.1 Single-Baseline Solution

The linearized double difference observation equations are collected in the following linear system of equations⁽¹⁾:

$$y = Bb + Aa + e \dots\dots\dots (5)$$

where y is the vector of observed minus computed double difference carrier phase measurements, $y \in R^m$; b is the vector that contains the increments of the p baseline coordinates; a is the vector of n double difference ambiguities; B is the $m \times p$ design matrix for the baseline coordinates; A is the $m \times n$ design matrix for the ambiguity terms; e is the vector of unmodelled effects and measurement noise.

The least-squares principle will be used to compute estimates for the baseline coordinates and the integer double difference ambiguities⁽⁷⁾:

$$\min_{b,a} \|y - Bb - Aa\|_{Q_y}^2 \text{ with } b \in R^p \text{ and } a \in Z^n \dots\dots\dots (6)$$

The parameter estimation is carried out in three steps: the float solution, the integer ambiguity estimation and the fixed solution.

In first step, the float solution, the equation (6) is carried out with $b \in R^p$, $a \in R^n$. The real valued estimates and variance-covariance matrix will be obtained⁽¹⁾:

$$\begin{bmatrix} \hat{a} \\ \hat{b} \end{bmatrix}, \begin{bmatrix} Q_{\hat{a}} & Q_{\hat{a}\hat{b}} \\ Q_{\hat{b}\hat{a}} & Q_{\hat{b}} \end{bmatrix} \dots\dots\dots (7)$$

The second step, the integer ambiguity estimation, consists of:

$$\min_a \|\hat{a} - a\|_{Q_{\hat{a}}}^2 \text{ with } a \in Z^n \dots\dots\dots (8)$$

This minimized yields the integer least-squares estimates for the vector of ambiguities: \tilde{a} . The computation of the integer estimate will be used LAMBDA method.

In the third step, the fixed solution, the final solution will be obtained with the ambiguities fixed to their integer least-squares estimates \tilde{a} ⁽¹⁾,

$$\tilde{b} = \hat{b} - Q_{\hat{b}\hat{a}} Q_{\hat{a}}^{-1} (\hat{a} - \tilde{a}) \dots\dots\dots (9)$$

The least-squares estimates \tilde{b} and \tilde{a} are the solution to the constrained minimization equation (6).

3.2.2 LAMBDA Method

The LAMBDA method⁽¹⁾ essentially consist of an efficient implementation of integer least squares esti-

mation, where part of the efficiency is caused by performing a decorrelating ambiguity transformation. The ambiguity search space can be defined by⁽⁷⁾,

$$\Omega_a = \{a \in Z^n \mid (\hat{a} - a)^T Q_a^{-1} (\hat{a} - a) \leq \chi^2\} \dots\dots(10)$$

with χ^2 a to be chosen positive constant. The boundary of this search space is ellipsoidal. It is centered at \hat{a} , its shapes is governed by the variance-covariance matrix Q_a and its size is determined by χ^2 . The search space is usually extremely elongated, due to the high correlations between the ambiguities. Since this extreme elongation hinders the computational efficiency of the search, the search space is first transformed to a more spherical shape⁽⁷⁾,

$$\Omega_z = \{z \in Z^n \mid (\hat{z} - z)^T Q_z^{-1} (\hat{z} - z) \leq \chi^2\} \dots\dots(11)$$

using the admissible ambiguity transformation $\hat{z} = Z^T \hat{a}$, $Q_z = Z^T Q_a Z$.

Since the bootstrapping estimator is so easy to compute and at the same time gives a good approximation to the integer least-squares estimator once properly decorrelated, the bootstrapped solution is an excellent candidate for setting the size of the ambiguity search space. Following the decorrelation step $\hat{z} = Z^T \hat{a}$, the LAMBDA method therefore uses the bootstrapped solution \tilde{z} for setting the size of the ambiguity search space as

$$\chi^2 = (\hat{z} - \tilde{z}_B)^T Q_z^{-1} (\hat{z} - \tilde{z}_B) \dots\dots\dots(12)$$

Using the triangular decomposition of Q_z , the left-hand side of the quadratic inequality in equation (11) is then written as a sum of squares⁽¹⁾:

$$\sum_{i=1}^n \frac{(\hat{z}_{iI} - z_i)^2}{\sigma_{iI}^2} \leq \chi^2 \dots\dots\dots(13)$$

Once the search has completed, one can either output the transformed integer least-squares solution \tilde{z} or, by using the inverse transform $\tilde{a} = Z^{-T} \tilde{z}$, output the integer least-squares solution of the original ambiguities.

More information about the LAMBDA method can be found in⁽¹⁾.

3.2.3 Ambiguity Success Rate

The ambiguity success rate is the probability, or chance, that the integer ambiguities are correctly estimated. It can be written in equation form as⁽⁴⁾

$$P(\tilde{a} = a) = \int_{S_a} p_a(x) dx \dots\dots\dots(14)$$

where $p_a(x)$ is the probability density function of the float ambiguities; S_a is the pull-in region, or area around the correct integer for which any float solution gets “pulled” towards the correct fixed solution. The ambiguity success rate depends on three contributing factors, the functional model, the stochastic model, and the chosen method of integer estimation. Changes in any one of these will affect the ambiguity success rate.

In general, the integral in equation (14) is difficult to evaluate, however in case of the bootstrapping estimator, the probability of correct integer estimation could be given explicitly as⁽⁷⁾:

$$P(\tilde{a}_B = a) = \prod_{i=1}^n \left[2\Phi\left(\frac{1}{2\sigma_{iI}}\right) - 1 \right] \dots\dots\dots(15)$$

where n is the number of ambiguities and

$$\Phi(x) = \int_{-\infty}^x \frac{1}{\sqrt{2\pi}} \exp\left\{-\frac{1}{2}v^2\right\} dv \dots\dots\dots(16)$$

The conditional standard deviations σ_{iI} can be obtained directly as the square-roots of the entries of the diagonal matrix D in the triangular decomposition of the variance-covariance matrix $Q_a = LDL^T$.

The ambiguity success rate can be evaluated once the functional model and stochastic models are known. Similar to the usage of dilution of precision measures, it can be computed without having the actual measurements available, that is, before actual field operation. By means of the success rate, the user is given a rigorous way of assessing how often one can expect ambiguity resolution to be successful. It has been proven that the integer least-squares estimator with the LAMBDA method has the largest success rate of all admissible integer estimators⁽¹⁰⁾.

4. Results and Analysis

In this section the expected performance of hybrid modernized GPS and Galileo positioning are analyzed for various scenarios in Japan. The scenarios include

GPS alone with dual and triple frequency, Galileo alone with dual and triple frequency and eventually integrated GPS and Galileo. First the model parameters and basic assumptions are briefly reviewed.

4.1 Set Up

In all computations it is assumed that the double difference ambiguities remain constant during the complete time span. To compute the positions of the GPS satellites and to simulate the positions of the Galileo satellites, a YUMA almanac was used, in the same way as was done for the integrated GPS-Galileo computations⁽²⁾. For 24 GPS satellites and 27 Galileo satellites constellations were used, continuously tracked at March 6, 2003, 12:00 for spatial variations and from March 6, 2003, 00:00 to March 7, 2003, 24:00, with a sampling interval of 120 seconds, for temporal variations. The receiver-satellite geometry was simulated over Japan for spatial variations and at Tokyo ($35^{\circ}39'59'' N$, $139^{\circ}47'32'' E$) for temporal variations. The visible satellites were masked by 15° cut-off elevation. The standard deviations of all phase and code observation were set at 0.003 m and 0.30 m, respectively. Three different baseline lengths, short baseline, medium baseline and long baseline, are considered. The short baseline is typically only of a few kilometers length, the medium baseline some tens of kilometers and the long baseline can be hundreds of kilometers. On the short baseline differential atmospheric delays are assumed to be completely absent (zero). These delays are to be accounted for on the medium and long baseline. A tropospheric zenith delay and ionospheric slant delays are included as unknown parameters, but the uncertainty in these parameters' values has been restricted. Variations in the delays are tolerated to a reasonable small extent on a medium baseline ($\sigma_T = 0.01m$ and $\sigma_I = 0.02m$), and to a much larger extent on a long baseline ($\sigma_T = 0.10m$ and $\sigma_I = 0.40m$)⁽⁵⁾. Single epoch solutions are considered, i.e. instantaneous positioning.

4.2 Spatial Variations

Before considering temporal variations performance of hybrid modernized GPS and Galileo, the spatial variations performances are analyzed.

Fig. 1, 2 and 3 show the GPS, Galileo and integrated GPS-Galileo visible satellite number with geo-

graphic location, respectively. The visible satellite

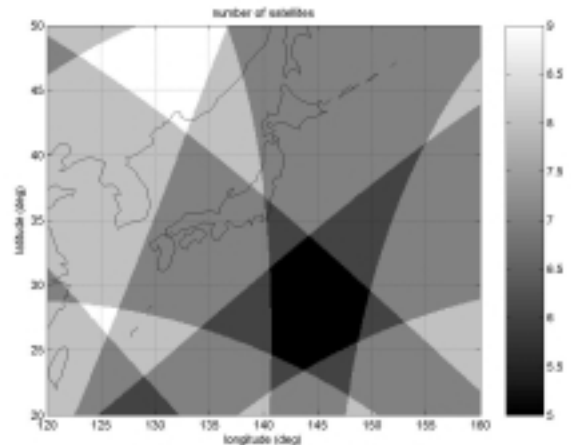


Fig. 1 Visible satellite number spatial variations (GPS)

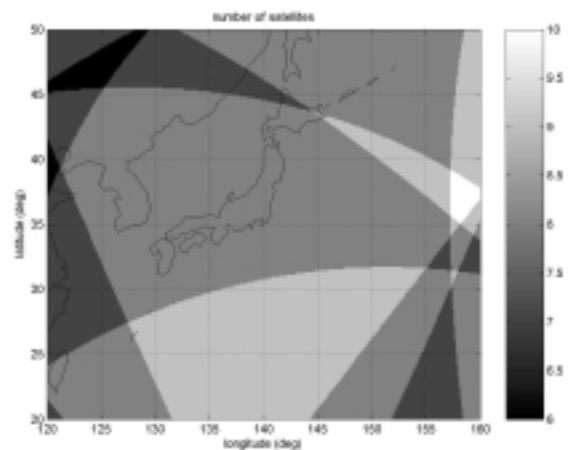


Fig. 2 Visible satellite number spatial variations (Galileo)

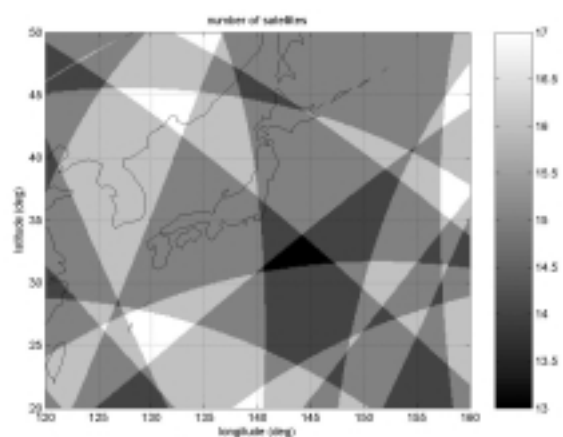


Fig. 3 Visible satellite number spatial variations (integrated GPS-Galileo)

number of GPS varies between 5 and 9. Galileo gives similar results with values between 6 and 10. If it was possible to use the integrated GPS and Galileo, the visible satellite number above 13 at any location could

be obtained.

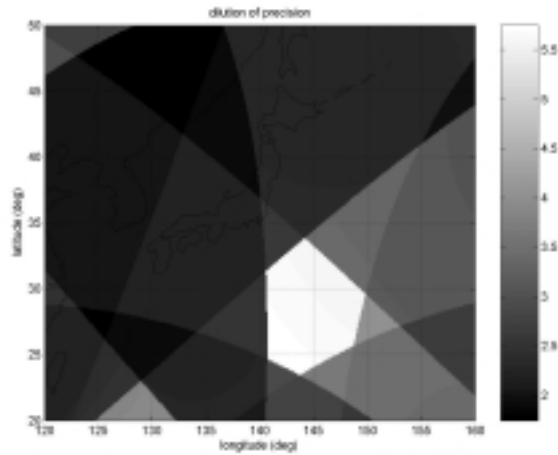


Fig. 4 GDOP spatial variations (GPS)

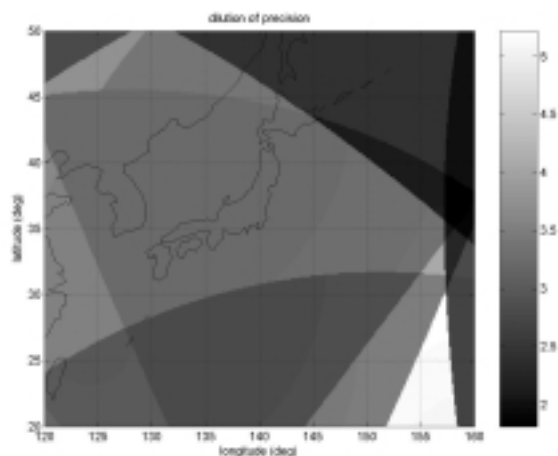


Fig. 5 GDOP spatial variations (Galileo)

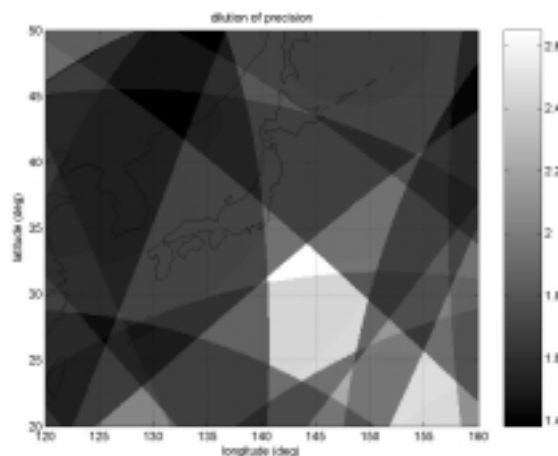


Fig. 6 GDOP spatial variations (integrated GPS-Galileo)

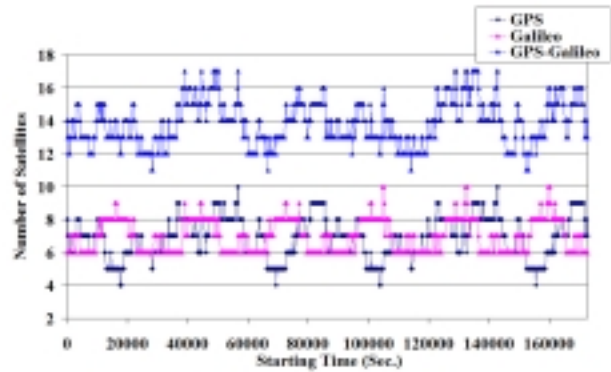


Fig. 7 Temporal variations of visible satellite number

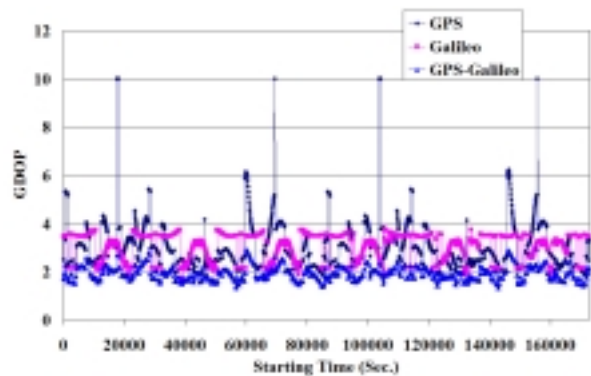


Fig. 8 Temporal variations of GDOP

Fig. 4, 5 and 6 show the spatial variations of GDOP for the GPS, Galileo and integrated GPS-Galileo, respectively. The GDOP of GPS varies between 1.74 and 5.74. Galileo gives similar results with values between 1.81 and 5.22. If it was possible to use the integrated GPS and Galileo, GDOP could be obtained between 1.38 and 2.65.

4.3 Temporal Variations

4.3.1 Visible Satellite Number and GDOP

Fig. 7 presents the variation of visible satellite number for the GPS, Galileo and integrated GPS-Galileo, over a full two days period. The satellite number of GPS varies between 4 and 10. Galileo also gives similar values between 6 and 10. The values of integrated GPS-Galileo are between 11 and 17.

Fig. 8 shows the GDOP of GPS, Galileo and integrated GPS-Galileo as a function of time. The GDOP of GPS varies between 1.67 and 10.00. Galileo gives values between 1.74 and 3.74. The values of integrated GPS-Galileo are between 1.30 and 2.94. The GDOP mean values of GPS, Galileo and integrated GPS-Galileo are 3.00, 3.03 and 1.90, respectively. Comparing Fig. 8 with Fig. 7, the user would immedi-

ately notice the jump in GDOP of GPS, when the number of GPS satellites drops to four.

4.3.2 Ambiguity Success Rate

Table 3 and Fig. 9 summarize the average ambiguity success rates of all scenarios.

4.3.2.1 The GPS Case

On the short baseline, the ambiguity success rates are 99.43% and 99.97% for dual and triple frequency, respectively. On the medium, the ambiguity success rates are improved from 90.93% to 95.78% by using triple frequency. From dual frequency to triple frequency yields an improvement from 13.62% to 25.01% for long baseline.

4.3.2.2 The Galileo Case

On the short baseline, the ambiguity success rates are 98.06% and 99.89% for dual and triple frequency, respectively. On the medium, the ambiguity success rates are improved from 89.95% to 95.78% by using triple frequency. From dual frequency to triple frequency gains only an improvement from 13.24% to 21.73% for long baseline.

4.3.2.3 The Integrated GPS and Galileo Case

On the short baseline, the ambiguity success rates are 100.00% and 100.00% for dual and triple frequency, respectively. On the medium, the ambiguity success rates are improved from 99.83% to 99.86% by using triple frequency. On the long baseline, ambiguity resolution is definitely not feasible using just a single epoch of data. From dual frequency to triple frequency yields only an improvement from 6.24% to 7.62% for long baseline.

Table 3 and Fig. 9 demonstrate that the ambiguity success rates decrease with increasing baseline length. On a short baseline, very high ambiguity success rate levels can be easily obtained. On the medium baseline, ambiguity success rate could be increased by tracking more satellites and improving satellite geometry. On the long baseline, it is difficult to resolve the ambiguities on the basis of just one epoch of data, neither with dual frequencies GPS, nor with triple frequencies integrated GPS-Galileo. The ambiguity success rates of integrated GPS and Galileo are not higher than for the two standalone systems. If, for example, GPS on its

Table 3 Ambiguity success rates of various scenarios (%)

Baseline Length		Short	Medium	Long
GPS	Dual	99.43	90.93	13.62
	Triple	99.97	95.78	25.01
Galileo	Dual	98.06	89.95	13.24
	Triple	99.89	95.87	21.73
Integrated GPS-Galileo	Dual	100.00	99.83	6.24
	Triple	100.00	99.86	7.62

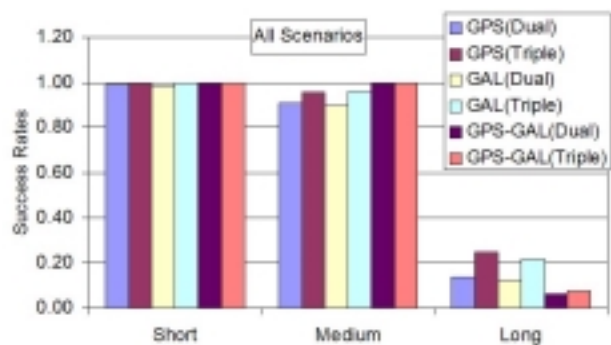


Fig. 9 Ambiguity success rates of various scenarios

own provides high success rates, addition of the Galileo observations may even result in slightly lower success rates.

5. Conclusion

In this article it has been shown that an integrated use of the new signals in space of the modernized GPS and the upcoming Galileo system will drastically improve the capability of RTK positioning in Japan. On a short baseline, very high ambiguity success rate levels can be obtained, even using a single epoch of data. On a medium baseline ambiguity success rate could be increased by the increased number of satellites and the improved satellite geometry. On long baseline, the instantaneous success rate is still too low for any practical applicability. Therefore for a future RTK system atmospheric, especially ionospheric, modeling is of utmost importance.

Acknowledgements

Discussion with Mr. Peter Joosten and Ms. Sandra Verhagen, Delft University of Technology, were very useful for understanding the LAMBDA algorithm.

References

- (1) de Jonge, P. and Tiberius, C. (1996): The

- LAMBDA method for integer ambiguity estimation: implementation aspects. LGR-Series 12, Delft Geodetic Computing Center, Delft University of Technology, The Netherlands, August 1996.
- (2) Eissfeller, B., Tiberius, C., Pany, T., Biberger, R., Schueler, T., and Heinrichs, G. (2001): Real-Time Kinematic in the Light of GPS Modernization and Galileo. In Proceeding of the 14th International Technical Meeting of the Satellite Division of the Institute of Navigation (ION GPS-2001), pp. 650–662, Salt Lake City, UT.
 - (3) Hein, G. and Pany, T. (2002): The European Satellite Navigation System Galileo. In Text for GPS Symposium 2002, pages 23–34, Tokyo, Japan.
 - (4) Joosten, P. and Tiberius, C. (2000): Fixing the Ambiguities - Are You Sure They're Right? GPS World, 11(5):46–51.
 - (5) Odijk, D. (2000): Weighting Ionospheric Corrections to Improve Fast GPS Positioning Over Medium Distances. In Proceeding of the 13th International Technical Meeting of the Satellite Division of the Institute of Navigation (ION GPS-2000), pp. 1113–1123, Salt Lake City, UT.
 - (6) Shaw, M., Turner, D. A., and Sandhoo, K. (2002): Modernization of the Global Positioning System. In Text for GPS Symposium 2002, pp. 3–12, Tokyo, Japan.
 - (7) Teunissen, P., Joosten, P., and Tiberius, C. (2002): A Comparison of TCAR, CIR and LAMBDA GNSS Ambiguity Resolution. In Proceeding of the 15th International Technical Meeting of the Satellite Division of the Institute of Navigation (ION GPS-2002), pp. 2799–2808, Portland, Oregon, 2002.
 - (8) Tiberius, C., Pany, T., Eissfeller, B., de Jong, K., Joosten, P., and Verhagen, S. (2002): Integral GPS-Galileo Ambiguity Resolution. In ENC-GNSS 2002 PROCEEDINGS, Copenhagen, Denmark.
 - (9) Verhagen, S. (2002a): Studying the Performance of Global Navigation Satellite Systems - A New Software Tool. GPS World, 13(6):60–65.
 - (10) Verhagen, S. (2002b): Performance Analysis of GPS, Galileo and Integrated GPS-Galileo. In Proceeding of the 15th International Technical Meeting of the Satellite Division of the Institute of Navigation (ION GPS-2002), pp. 2208–2215, Port-

Portland, Oregon, 2002.

Questions and Answers

Kazuaki Hoshinoo (Electronic Navigation Research Institute, Independent administrative Institution): Three different baseline, short baseline, medium baseline and long baseline, are considered. How long are the short baseline, medium baseline and long baseline?

Falin Wu: The short baseline is typically only of a few kilometers length, the medium baseline some tens of kilometers and the long baseline can be hundreds of kilometers.

Kazuaki Hoshinoo (Electronic Navigation Research Institute, Independent administrative Institution): On the long baseline, why are the ambiguity success rates of integrated GPS and Galileo not higher than for the two standalone systems?

Falin Wu: Because the ambiguity success rate depends on three contributing factors, the functional model, the stochastic model, and the chosen method of integer estimation. Changes in any one of these will affect the ambiguity success rate. There are more unknown ambiguities for integrated GPS and Galileo than GPS or Galileo standalone system. The effects of the larger number of unknowns may offset the improvement due to better geometry.

Nobuaki Kubo (Tokyo University of Mercantile Marine): In computation, the standard deviations of the all phase and code observation were set at 0.003 and 0.30m, respectively. How do you deal with the multipath in your research?

Falin Wu: Multipath is the error caused when the signal arrives at the receiver via more than one path, normally caused by reflections near the receiver. As a result, it is highly dependent upon the conditions surrounding the receiver antenna, the type of antenna that is used, and the internal tracking loop algorithms of the receiver. Because there is no model that can be used for the general case, the multipath hasn't been taken into account in this study.